

# ESTIMATION OF TRANSMITTED LOADS USING EXPERIMENTAL SUBSTRUCTURING

**Mathieu Corus<sup>†</sup>, Olivier Sauvage<sup>‡</sup>, Etienne Balmès<sup>†</sup>**

<sup>†</sup> ECP, MSSMat, Grande Voie des vignes, 92295 Châtenay-Malabry, France

<sup>‡</sup> PSA Peugeot Citroën - route de Gisy, 78943 Vélizy-Villacoublay Cedex- France

mathieu.corus@edf.fr - olivier.sauvage@mpsa.com - balmes@sdtools.com

## Abstract

Predicting the in operation behaviour of complex assembly including active components is a challenge, since accurate models of those components are rarely available. For example, the dynamic effects of injectors bolted on a cylinder head are of critical interest, but difficult to predict in the design phase. Indeed, manufacturers do not provide a description of the internal behaviour of the injector. The physical injectors and a FE model of the cylinder head are the data available.

This paper presents a method to estimate an equivalent load applied by an active component on a given structure. First, a statically complete dynamic model of the active component is set up, using a test device reproducing the joints between the active component and the target structure. Since a tuned FE model of this test device is available, data expansion and model reduction techniques are used to compute residual flexibilities for active component test model. Next, a component-dependent equivalent load is identified. Then, test and FE models are combined to compute the forces to apply on the target structure.

A numerical example summarizes the methodology and highlights the practical implementation. Good results are obtained with realistic simulation data. Results also illustrate practical difficulties and limitations.

## 1 Introduction & context

Force identification is a key step in the design procedure of efficient structures. It is mainly conducted on test devices that aim to be representative of the final structure. In the design phase, it can be critical to have a proper estimate of the loads that will act on the structure. In particular, when those loads derive from a connected substructure, interaction between components is of critical interest. However, the behaviour of the active component is unknown most of the time.

This is typically the case when a car manufacturer needs to design a new cylinder head, including injectors. Injectors are active structures, whose behaviour is only known precisely by another manufacturer, but that can have big consequences on the dynamics of the whole engine. In order to be able to predict the behaviour of that engine under injection loads, one must then identify both the internal loads, and a realistic model of the injector, assuming that a tuned model of the cylinder head exists. In this paper, a method is introduced to achieve these two goals. First, a method allowing to set up a statically complete model of the active component (injector, in our case) is proposed. In a second step, the determination of an equivalent load, taking the behaviour of the active device into account, to be applied on the target structure (i.e. cylinder head) is presented.

The need for a statically complete model of the active component is critical. Active component are coupled to different substructures, and the estimation of the coupled dynamic behaviour is highly linked to a good estimation of the residual flexibilities associated to the joint ([1, 2]). Some authors already proposed different techniques to estimate residual flexibilities ([3, 4, 5]), but they all impose a discretization of the coupling interface, and measurements on the interface DOF, which is not always realizable.

When more complex joints are involved, such as the one described figure 1, such techniques become impracticable, and one may find some other way to tackle the problem. To overcome this major difficulty, a third structure is introduced. Using this test bed, two test will be conducted. Combined use of model reduction and data expansion techniques on the tuned F.E. of the test bed on one hand, and a rough F.E. model of the active component on the other hand, will lead to an accurate estimation of the useful components of the residual flexibilities. The use of different tests has already been proposed, in [6] for example, but the novelty lies in the ability not to measure anything at the coupling interface.

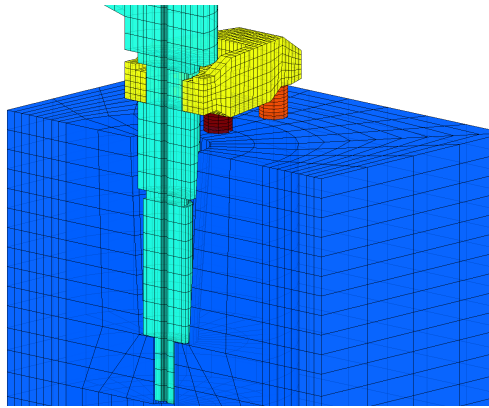


Figure 1: Example of complex bond realization. Active device (clear blue) is maintained in contact with the test bed (dark blue) by the mean of a fork (yellow) resting on a centring dot (orange) and tightened with a screw (dark red).

The second major step is the set up of a generalized load defined on the active component inducing the same effects on the test device and on the target structure that the "true" internal loads, assumed to be unknown and unreachable. Inverse problem based on in operation measurements and tuned F.E. model of the test bed is solved, using techniques presented in [7], to determine an equivalent loading on the coupling interface. Then, using the statically complete model of the active structure, a generalized load applied to the active component is computed. A coupled model of the target structure and the active component is built and submitted to the previously computed generalized load. Finally, an equivalent load including the behaviour of the active component is computed.

We assume that all those structure will have a linear behaviour, and only consider the low frequency band (with respect to the dynamics of the structures), so that reduced modal models can be used. We use the following notations :

- $\Omega$  denotes the unknown structure to be identified (i.e. injector),
- $\Omega_0$  denotes the well known test device (i.e. test cubic bloc),
- $\Omega_1$  denotes the target structure (i.e. cylinder head),
- $\Omega + \Omega_0$  (resp.  $\Omega + \Omega_1$ ) denotes the assembled structure of  $\Omega$  linked to  $\Omega_0$  (resp.  $\Omega_1$ ),
- $\Sigma$  denotes the boundary where  $\Omega$  is linked to the other substructures. In both cases, this boundary is supposed to have the same geometry, and the joint is supposed to be realized the same way.
- $\partial\Omega$  denotes the (unknown) boundary where internal loads are supposed to act.
- $f$  denotes the internal loads. They are assumed not to depend on the coupling with other substructure.
- $f_0$  (resp.  $f_1$ ) denotes the equivalent loads to be applied on  $\Sigma$  to induce the same response in  $\Omega_0$  (resp.  $\Omega_1$ ) that  $f$  applied to  $\Omega + \Omega_0$  (resp.  $\Omega + \Omega_1$ ) on  $\partial\Omega$ ,
- $\tilde{f}$  denotes the equivalent generalized loads defined in  $\Omega \setminus \Sigma$  inducing the same effects on  $\Omega_0$  and  $\Omega_1$  than  $f$  applied on  $\partial\Omega$ .

The thick lines of the whole process are summarized on the figure 2 :

- Set up a statically complete model of the active component:
  - set up a relevant expansion basis using a free interface local FE model of the active device,
  - build a reduced basis of static correction shapes, filtered with respect to the free interface modes of the active component,
  - build a FE assembled model using the FE model of the test device and the statically complete model of the active component, introducing arbitrary stiffness contribution for the correction shapes,
  - tune these stiffness contributions comparing test and numerical results on the assembled structure  $\Omega + \Omega_0$ .
- Build the equivalent loads  $f_0$  between the test device and the active component :
  - set up a proper expansion basis, based on the FE model of the test device,
  - extend the eigen modes of the test device using this basis,
  - extend in-operation measurement of the test device + active component assembly on this same basis.
  - derive the generalized loads  $f_0$  using the extended measurements.

- Compute the generalized interface load  $\tilde{f}$  :
  - interface load  $f_0$  is known, and interface displacements can be derived from expansion process. Under these assumptions,  $\tilde{f}$  is derived from relation (22).

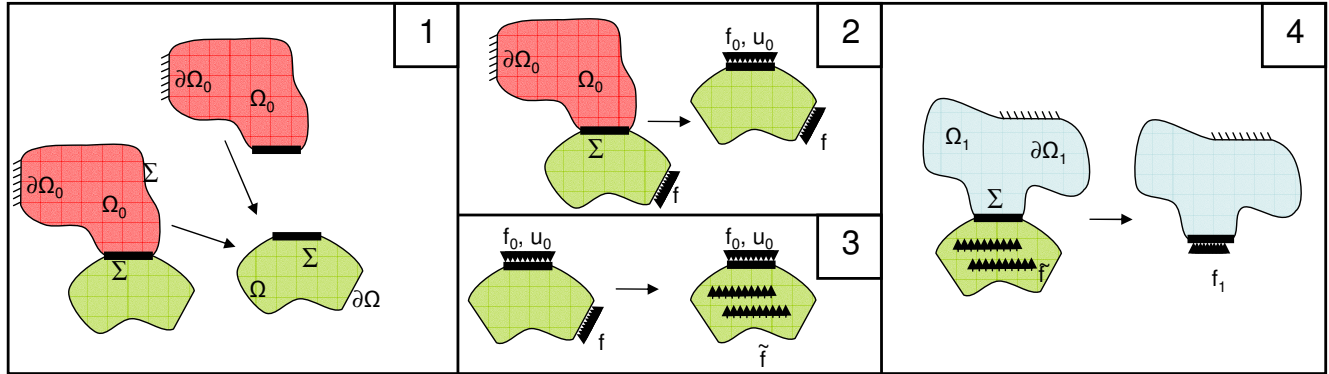


Figure 2: Summary of the method.

## 2 Statically complete reduced model deriving from tests

The set up of a statically complete model is the key of the success of the proposed methodology. Indeed, its role is critical in the definition of the generalized load, and in the estimation of the behaviour of the target structure, when coupled to the active component. The technique, developed in the following, stands on the combination of modal test results, reduced model substructuring and data expansion on a rough F.E. model of the active device.

In the first section, reduced model substructuring methods are summarized. In the second part, it is shown how the coarse F.E. model of the active component is used to define a generalized set of residual flexibilities. Various proposals are made, depending on the boundary conditions of the complete sucture assemblies. The relationship leading to the optimal residual flexibility set is then given in the third section.

### 2.1 Reduced model substructuring

Component mode synthesis (CMS) is now widely known, and used to reduce the size of F.E. models for computation purposes. It is also a usefull tool originally developed to deal with experimentally oriented coupling. Main relationships are reminded using a two components example. First, assume that each component has been modeled using F.E. techniques. Let  $Z$  denote the dynamic stiffness of the active structure (resp.  $Z^0$  for the test device),  $q$  (resp.  $q_0$ ) the displacements and  $f$  the discretized forces. Let  $C$  (resp.  $C^0$ ) be the ouput and  $B$  (resp.  $B^0$ ) the input shape matrices associated to the interface DOF.  $B_{ext}$  (resp.  $B_{ext}^0$ ) is the input shape matrix associated to external loads. For each structure, one has the following relations of evolution and observation :

$$\begin{cases} [Z] \{q\} = [B] \{u\} + [B_{ext}] \{u_{ext}\}, \\ \{y\} = [C] \{q\}, \end{cases} \quad (1)$$

where  $y$  (resp.  $y^0$ ) denotes the interface displacements,  $u$  (resp.  $u^0$ ) the interface loads, and  $u_{ext}$  (resp.  $u_{ext}^0$ ) the external loads.

Assuming the components are perfectly linked on the interface, the continuity of the displacements is written

$$[C - C^0] \begin{Bmatrix} q \\ q^0 \end{Bmatrix} = 0, \quad (2)$$

and the nullity of the virtual work (generally called principle of action and reaction), for all the displacements fields  $q$  and  $q^0$  verifying (2), gives

$$([C] \{q\})^T ([B] \{u\}) + ([C^0] \{q^0\})^T ([B^0] \{u^0\}) = 0. \quad (3)$$

Let  $[R^T (R^0)^T]^T$  denote a basis of the nullspace of  $[C \ -C^0]$ . Hence, for each  $\{q; q^0\}$  verifying equation (2), there exist a unique vector  $q_r^{\&0}$  verifying

$$\begin{Bmatrix} q \\ q^0 \end{Bmatrix} = \begin{bmatrix} R \\ R^0 \end{bmatrix} \{q_r^0\}. \quad (4)$$

Substituting in (3) using (4) and evolution relationships leads to the coupled problem

$$\left[ R^T Z R + (R^0)^T Z^0 R^0 \right] \{q_r^0\} = \quad (5)$$

$$\left[ R^T B_{ext} \right] \{u_{ext}\} + \left[ (R^0)^T B_{ext}^0 \right] \{u_{ext}^0\}. \quad (6)$$

### 2.1.1 reduced models

One may then do the assumption that, for each substructure, a particular basis  $T$  (resp.  $T^0$ ) can represent the dynamic behaviour over a given frequency range. Once the basis is built, generalized displacements field  $\eta$  gives a good estimate of the whole behaviour. They are related to FE DOF  $q$  through the relationship

$$\{q\}_N = [T]_{N \times N_g} \{\eta\}_{N_g}, \quad (7)$$

where subscripts  $N$  denote the size of the complete F.E. model,  $N_g$  the size of the reduced subset of generalized DOF and  $N_g \ll N$ .

Introducing the continuity of the generalized interface displacement, and null virtual work of the generalized forces, the coupled reduced system takes the form

$$\begin{aligned} & \left[ (T R_r)^T Z (T R_r) + (T^0 R_r^0)^T Z^0 (T^0 R_r^0) \right] \{\eta_r^{\&0}\} = \\ & \left[ (T R_r)^T B_{ext} \right] \{u_{ext}\} + \left[ (T^0 R_r^0)^T B_{ext}^0 \right] \{u_{ext}^0\}. \end{aligned} \quad (8)$$

### 2.1.2 generalized rigid link between substructures

One of the major advantage of the evolution / observation formulation is the ability to easily take various coupling conditions into account. Indeed, coupling two structures using all the DOF describing the behaviour of the interfaces can lead to unrealistic predictions, bonding too much the motion. This approach is a major tool when the complexity of the coupling condition is involved, hence allowing the use of generalized coupling condition, that is easier to take into account [8]. One can easily build generalized motion for each interface, and then directly derive a basis for the kernel of the coupling operator.

#### - Output shape matrix

In most case, interfaces are described using a large number of DOF, when the overall displacements can be represented using a much lower number of generalized DOF. In particular, when the coupling areas are small with respect to the sizes of coupled structures, we can assume that six DOF associated to the rigid body motion of the interfaces are involved. This way, we can define  $C_{I-rb}$  as a pseudo inverse of those rigid body modes, restrained on the interface DOF. Hence, we will use

$$[C_{I-rb}] = [\Phi_{I-rb}]^+ [C_I]. \quad (9)$$

Since the number of finite element DOF describing the interface is larger than the number or rigid body modes of the interface, the relation (9) leads to a well conditioned problem.

#### - Input shape matrix

The definition of  $C_{I-rb}$  allows the projection of any interface motion onto interface rigid body modes. To define the associated input shape matrix  $B_{I-rb}$ , it is convenient to consider the dual quantities of the generalized displacements of the interface. Hence, the expression of  $B_{I-rb}$  is straightforward, since we have

$$[B_{I-rb}] = [C_{I-rb}]^T. \quad (10)$$

- Null subspace basis

For the case of the generalized rigid body motion of the interfaces, let  $[(R_{rb})^T (R_{rb}^0)^T]^T$  denote a basis of the nullspace of  $[C_{I-rb}T - C_{I-rb}^0T^0]$ . So, there is a unique vector  $\eta_{rb}^0$  representing the whole behaviour for each state  $\{\eta; \eta^0\}$ , and we have

$$\begin{Bmatrix} \eta \\ \eta^0 \end{Bmatrix} = \begin{bmatrix} R_{rb} \\ R_{rb}^0 \end{bmatrix} \{\eta_{rb}^0\}. \quad (11)$$

## 2.2 Generalized flexibility reconstruction

This section presents the key feature to ensure good equivalent load estimation. No tuned FE model is available for the active component. Since it would be expensive and time consuming to build one, we will seek to use a mixed numerical / experimental approach. The reduction basis adopted for the active component stands on a set of free-interface modes, and needs to be augmented with a subset of generalized flexibility correcting modes.

These vectors hence contain two informations. The shape of the deformed model under a given load, and the scaling between the amplitude of displacements and the load. In the first section, the construction of generalized correction modes shapes is proposed. This step stands on a coarse FE model of the active structure. In the second section, the scaling to the proper mechanical behaviour of the active component is presented. To achieve scaling, modal analysis of both test structure and test and active coupled structures are used, in conjunction with data expansion techniques.

### 2.2.1 Generalized correction shapes

The first step to the set-up of a well conditioned statically complete representation of the active device is the definition of relevant shapes. These shapes must consistently represent the displacements over the active device for all the interface loads. A local FE model, a concept already presented in [9], is introduced. The main aim of this rough FE modal is to built a kinematical relationship between the measurement points and the interface DOF. As stated before, building a tuned FE model of the structure is not acceptable. This FE model of the instrumented sub domain includes reasonable mechanical properties. This choice has many advantages :

- obtain a quick design and set up of a model depicting the geometry of the active structure,
- ease the construction of smooth displacements fields defined at measurement points and on the interface,
- ensure the regularity of the shapes with respect to the equation of motion.

Moreover, a quick tuning procedure can be set up, so that the first few modes shapes of the local model reasonably match the identified mode shapes of the active component, ensuring the correctness of *a priori* computed correction shapes. Let  $M^L$  and  $K^L$  denote the mass and stiffness matrix of the local model, and  $q^L$  the FE DOF.

This FE model is then used to defined a subset of generalized correcting shapes, as it would be in classical CMS methods. Since we chose to use generalized links between substructures, the equations defining the main correction shapes  $T_{gcs}$  need to be adapted. These shapes, as presented in [10], are :

- generalized constraint modes,
- generalized residual inertia relief modes,
- generalized attachment modes.

Since the range of constraint modes (+ residual inertia relief) modes equals the range of attachment modes (+ rigid body) modes, reorthogonalisation procedure can be used, so that the choice of a subset or an other has no importance. It is also the case with generalized correction shapes. In the following,  $T_{gcs}$  will be built using constraint modes (+ residual inertia relief modes) for convenience.

### 2.2.2 Tuning of generalized correcting modes

The correction shapes have been built thanks to the local FE model of the active device. Since its geometry and overall mechanical properties are relevant with the real structure, computed shapes should give a good estimation of the expected shapes. However, this local FE model is not tuned at all, so these correction shapes can not be used directly, and therefore need tuning. To achieve this goal, two different modal analyses will be conducted.

The first one is the modal analysis of the active component alone. A set of identified modes  $\Phi_t$  is identified, along with natural frequencies  $\omega_t$  and damping ratios  $\xi_t$ . This test enables the quick tuning of the local model, which is used to compute the correction shapes, and that will also be used to set up a statically complete basis with independent vectors. The second modal analysis is conducted on the test device and the active component, and will directly be used to tune the scales of the correcting shapes. Let  $\Phi_t^{\&0}$ ,  $\omega_t^{\&0}$  and  $\xi_t^{\&0}$  denote the identified mode shapes, natural frequencies and damping ratios for the assembled structure  $\Omega + \Omega_0$ .

- *Statically complete reduced model of the active component*

Once the first modal analysis is performed, and the local FE model is properly set up, we can define a statically complete reduction basis for the active structure. This basis contains the set of  $n_t$  free interface experimental modes  $\Phi_t$ , and the correction shapes  $T_{gcs}$ . Since  $\Phi_t$  is defined at measurement points, and  $T_{gcs}$  is defined for the  $q^L$ , let denote  $C_t^L$  the output shape matrix allowing the observation of measurements points from local FE DOF. Hence, the vectors  $[\Phi_t \ C_t^L T_{gcs}]$  are all defined at measurement points, and are relevant to set up a correct reduced model. However, vectors of  $\Phi_t$  and  $T_{gcs}$  can be strongly collinear, and then  $T_{gcs}$  must be filtered to remove any free interface mode contribution.

To achieve this goal, vectors of  $\Phi_t$  are extended on the whole local model. Let denote  $T_t^L$  the expansion basis. It derives from a set of orthonormalized attachment modes defined over the local FE model. Vectors of  $T_t^L$  are sorted with respect to their strain energy. A truncated basis will be used in the expansion process, allowing the control of both regularity and efficiency of the expansion procedure. This issue has been extensively discussed in [9]. Hence, extended mode shapes  $\Phi_t^L$  are given by

$$[\Phi_t^L] = [T_t^L] [\eta_t^L], \quad (12)$$

$\eta_t^L$  being the solution of the least square problem defined by

$$[\eta_t^L] = \underset{\eta^L}{\text{ArgMin}} \left( \left\| [C_t^L] [T_t^L] [\eta^L] - [\Phi_t] \right\|^2 \right). \quad (13)$$

The basis  $\Phi_t^L$  is then defined on local model DOF, and it can then be used to filter the correction shapes. The complete basis  $[\Phi_t^L \ T_{gcs}^L]$  is then orthonormalized with respect to  $M^L$  and  $K^L$ . At this stage, the quick tuning of the local model is important, since the  $n_t$  first vectors of the orthonormalized basis must span the same subspace than  $\Phi_t^L$ , even if the vectors can not properly be paired. It is a critical condition to ensure the proper filtering of  $T_{gcs}^L$ . Let denote  $T_r^L$  the filtered basis based on  $T_{gcs}^L$ .

- *Tuning correction using coupled mode shapes*

The new basis  $[\Phi_t^L \ T_r^L]$  then contains all the information concerning the shape of the vectors. However, since the local FE model is not a completely tuned FE model of the active component, one can not ensure the scaling of  $T_r^L$ . Scales  $\omega_r^L$  of vectors  $T_r^L$  are defined using the orthogonality relations :

$$\begin{cases} [T_r^L]^T [M^L] [\Phi_t^L] = [0], \\ [T_r^L]^T [M^L] [T_r^L] = [Id], \\ [T_r^L]^T [K^L] [T_r^L] = [\tilde{\omega}_r^L]^2. \end{cases} \quad (14)$$

The stiffness contributions  $\tilde{\omega}_r^L$  will then be tuned using the modal analysis of the complete structure. Indeed, building a reduced model of the assembled structure  $\Omega + \Omega^0$  using the reduction basis  $[\Phi_t^L \ T_r^L]$  leads to

$$\left( -\tilde{\omega}_r^{\&0} [Id] + \left( [R_r]^T \begin{bmatrix} \omega_t^{\&0} & 0 \\ 0 & \tilde{\omega}_r^{\&0} \end{bmatrix} [R_r] + (T^0 R_r^0)^T K^0 (T^0 R_r^0) \right) \right) \{ \tilde{\Psi}_r^{\&0} \} = \{ 0 \}, \quad (15)$$

where  $\tilde{\Psi}_r^{\&0}$  and  $\omega_r^{\&0}$  denote the eigenmodes and eigenfrequencies of the coupled problem. We will then compare the predicted results with the measurements. The best stiffness contributions  $\omega_r^L$  should allow the most accurate prediction of the coupled behaviour ( $\tilde{\Phi}_t^{\&0}$ ,  $\tilde{\omega}_r^{\&0}$ ). Thus, a reduced model of the active device is available, and statically complete with respect to interface generalized loads.

### 3 Generalized loads identification

Once a complete reduced model of the active device is built, we can set up a generalized load that will have the same effects on  $\Omega_1$  that the true loads, that are impossible to determine, not knowing the exact behaviour of the active component. This process is divided into two parts. The first part is a classical force identification process. Having a tuned FE model of the test device, in operation measurements made on the assembled structure  $\Omega + \Omega_0$  are used to define a set of generalized interface loads  $f_0$  applied to the coupling boundary  $\Sigma$ . In the second part, these generalized interface loads are derived into generalized loads  $\tilde{f}$  defined all over the active structure, excluding DOF involved in the interface motion.

#### 3.1 Generalized interface equivalent loads

The first step is to identify generalized equivalent interface loads. Considering relation (8), and considering that external loads are only applied to the active device, it is obvious that the test device is only submitted to interface loads. Let denote  $f$  the true generalized external load. Thus, we have

$$\{f\} = [T^T B_{ext}] \{u_{ext}\}. \quad (16)$$

Hence, knowing the overall motion of the test device in operation, including the interface, directly leads to the expression of  $f_0$ .

$$\begin{cases} [(T_g^0)^T Z^0 T_g^0] \{\eta_t^0\} = - [T^T Z T] \{\eta\} + \{f\} = \{f_0\} \\ [C_{I-rb}^0 T_g^0 - C_{I-rb} T] \begin{Bmatrix} \eta_t^0 \\ \eta \end{Bmatrix} = \{0\}. \end{cases} \quad (17)$$

Identification of  $f_0$  can be done using classical inversion techniques, but one must be really careful, since results strongly depends on the techniques used. Indeed, since  $f_0$  must be 0 outside the interface, modelling and measurements errors, along with necessary regularization techniques will lead to a generalized load defined over the whole test device. A generalized inversion technique, proposed in [7], will be used to define the generalized interface loads.

In operation measurements  $y_t^{\&0}$  for the assembled structure are extended on a reduction basis  $\Phi^{\&0}$ . The vectors of  $\Phi^{\&0}$  are the normal modes of the assembled structure. For each frequency of interest, the motion defined on the FE DOF  $y^{\&0}$  is given by

$$\{y^{\&0}\} = [\Phi^{\&0}] \{\eta_t^{\&0}\}, \quad (18)$$

where generalized in operation DOF  $\eta_t^{\&0}$  are given by

$$\{\eta_t^{\&0}\} = \underset{\eta_t^{\&0}}{ArgMin} | [C_t^{\&0} \Phi^{\&0}] \{\eta^{\&0}\} - \{y_t^{\&0}\} |^2. \quad (19)$$

Let denote  $C_0^{\&0}$  the output shape matrix allowing the observation of the test device FE model from the assembled structure model. In operation motion being defined for the test device, the generalized interface loads  $f_0$  are directly given by

$$\{f_0\} = [Z^0] [C_0^{\&0}] [\Phi^{\&0}] \{\eta_t^{\&0}\}. \quad (20)$$

#### 3.2 Generalized equivalent load

Generalized interface loads being defined on the test device, the last step is the definition of an equivalent generalized load  $\tilde{f}$  on the active device. We seek a load that would have on  $\Omega_0$  exactly the same effects than the true load  $f$ . Assuming such  $\tilde{f}$  exists, it would then verify

$$\begin{cases} [(T_g^0)^T Z^0 T_g^0] \{\eta_t^0\} + [T^T Z T] \{\tilde{\eta}\} = \{\tilde{f}\}, \\ [C_{I-rb}^0 T_g^0 - C_{I-rb} T] \begin{Bmatrix} \eta_t^0 \\ \tilde{\eta} \end{Bmatrix} = \{0\}. \end{cases} \quad (21)$$

Displacements  $y_t^0 = [T_g^0] \eta_t^0$  on  $\Omega_0$  are the same, but displacements on  $\Omega$  may be different, since only generalized interface motion is constrained.

Substituting equations (17) and (21) gives the expression of the generalized load  $\tilde{f}$

$$\begin{cases} [T^T Z T] \{\tilde{y}\} = \{\tilde{f}\} - \{f_0\}, \\ [C_{I-rb}^0 T_g^0 - C_{I-rb} T] \begin{Bmatrix} \tilde{\eta}_t^0 \\ \tilde{\eta} \end{Bmatrix} \end{cases} \quad (22)$$

Equation (22) is then solved for each frequency step to set up the generalized load  $\tilde{f}$ .

## 4 Numerical example

In this section, a numerical experiment is built to validate the methodology previously defined and summarize the different steps. Simple FE models representing the test device, the active component and the target structure are given. Test results (EMA & in operation) for the test device & active component assembly are simulated. The main steps of the whole process are :

1. Identify a statically complete model of  $\Omega$  using various test configurations
2. Using in-operation measurement, determine the equivalent loads  $f_0$  on  $\Sigma$ .
3. Define a generalized load  $\tilde{f}$  on all  $\Omega \setminus \Sigma$  inducing the same loads and displacements on  $\Sigma$  than  $f$
4. Compute the behaviour of the assembled model  $\Omega + \Omega_1$  using the generalized load  $\tilde{f}$ , and derive the equivalent load  $f_1$  to be applied to  $\Omega_1$  on  $\Sigma$

For the purpose of the demonstration, generalized interface loads  $f_1$  deriving from  $\tilde{f}$  for the assembled structure will be compared to the "true" generalized load computed using the assembled FE model of the active component coupled to the target structure.

### 4.1 FE models and hypotheses

The purpose is to validate the reconstruction of a statically complete FE model of a structure only known experimentally, and then derive the generalized loads this structure can transmit to another. This example is fully numerical, but is conducted the way it would be in a real life situation. FE models of a test device, an active component, and the target structure are built. The coupling conditions between these models are much simpler than for the models presented on the figure 1. The coupling area is limited to the bottom face of the active device, involving a limited number of nodes. A generalized rigid body motion is assumed for both sides of the interface. The assemblies representing the assembled structures  $\Omega + \Omega_0$  and  $\Omega + \Omega_1$  are presented figure 3.

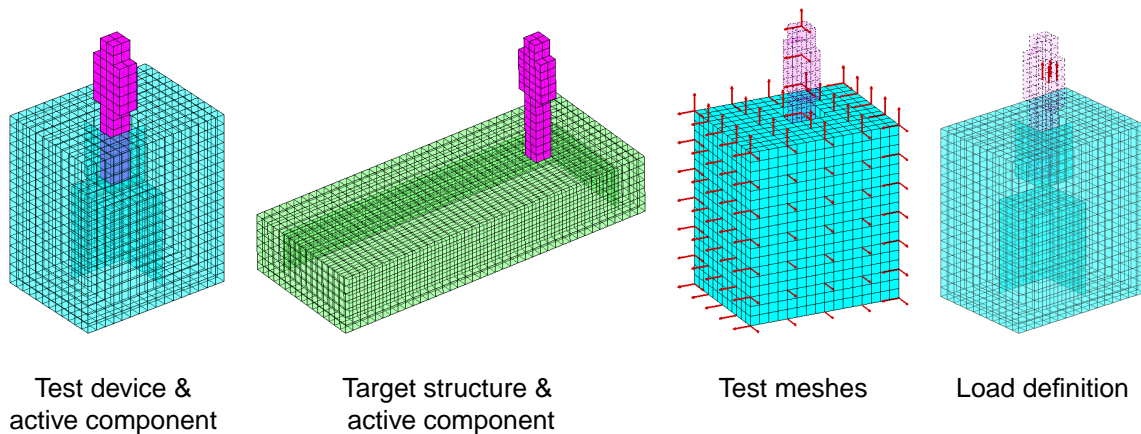


Figure 3: FE model assemblies, test meshes and load case used in the numerical test study.

To simulate the test results, experimental meshes are defined for the test device and the active component. These meshes are represented figure 3. All assemblies are supposed to be tested resting on a soft suspension,

simulating free free conditions. Hence, only five of the faces of the test device are available for measurements. Only out of plane accelerations are measured, using 164 sensors. The active component is tested using ten sensors combined in pairs in the plane of its cross section, in addition with a eleventh sensor measuring the acceleration of the upper cross section in the vertical direction. This rough configuration is used to represent the realistic test case that will be used to experimentally validate the methodology.

The load is defined to represent a realistic in operation behaviour. A load is applied in the z-direction (the vertical one), and is slightly uncentred to induce small loads in the other directions. The x direction corresponds to the longest in-plane direction for the test device, and the y direction the shortest one. We will test the ability of the proposed method to extract the essential information, here the z-directed load and torques along the x and y directions. This loading case is represented on figure 3. To represent the behaviour of the active component in the real application, a frequency band-limited impact is imposed to the structure. This assumption allows the use of Fourier transform of signals, instead of cross and inter spectra, since a phase reference is available for each measurement.

The study will be conducted on the [0 - 15kHz] frequency range, considering the final application and the stiffness of the various structure. The test device is assumed to be as stiff as possible, while the target structure is much more flexible. The active component is assumed to be designed as a stiff body including only few moving pieces, hence having only few modes within the given frequency range. References results have been computed using complete models of assemblies, assuming 1% of modal damping. Experimental modal analyses have been conducted overall the frequency range, and every mode within this frequency range is supposed to be properly identified. This assumption is relevant, considering that this includes the first fifteen modes for the test device, and only the first five modes for the active component.

## 4.2 Reconstruction of the correction shapes flexibilities.

This study is conducted using experimental models of the structure. Fifteen modes are available for the test device, five for the active component. A tuned FE model is available for the test device, hence statically complete model of this structure can easily be built. Correcting modes shapes for the active device are build according the description given in section 2.2.1, using the FE model presented in the figure 3. Since we are interested in overall behaviour, correction shapes are build considering generalized rigid body motion of the coupling interface. Hence, six correction shapes are built, using generalized inertia relief modes shapes definition. These shapes are orthonormalized with respect to the five flexible modes already available and the six computed rigid body modes. The figure 4 presents the results for the reference coupled model, and the result of the optimization procedure. The reference model is the complete FE model of the assembly. The reference coupled model is built using the statically complete model of the test device, including fifteen flexible modes shapes, the first five flexible modes of the active component, and the generalized correction, which flexibilities are computed using the FE model. The same flexible modes are used to compute the optimal flexibilities.

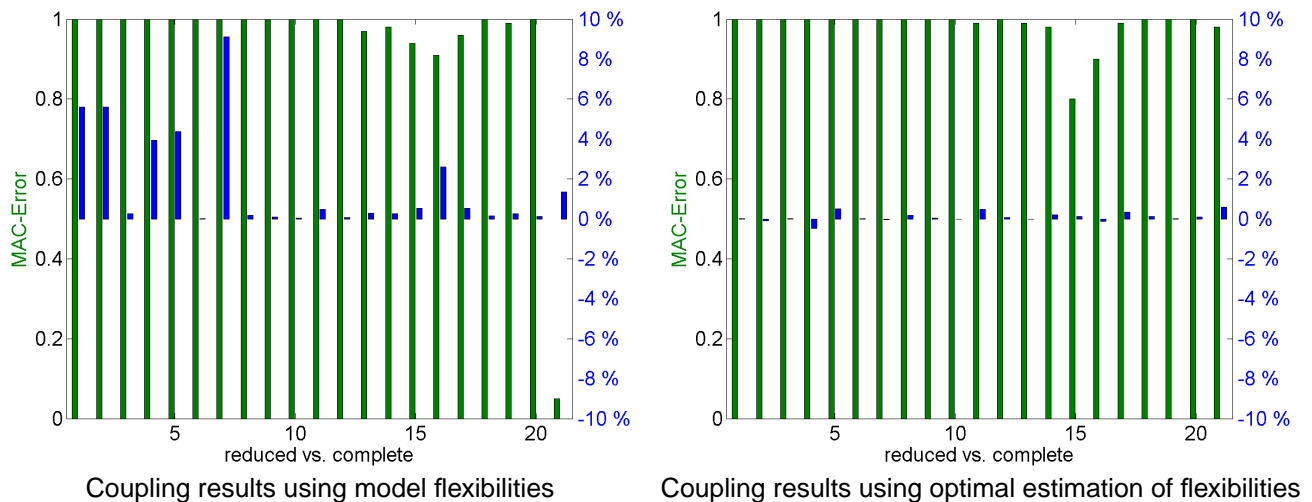


Figure 4: MAC and frequency relative errors for the real flexibilities (left) and the optimal result (right).

Since the complete basis is orthonormalized, the starting point for the generalized flexibilities should be higher than the last flexible frequency  $f_{max}$  of the active component. The six starting points for the optimization process are chosen to verify this assumption, and are adjusted to ensure a good convergence of the minimization process. The choice of this starting point is of critical importance. The minimization function focuses on the first 10 modes, including criteria on both MAC and frequencies. Both criteria are weighted to have an equal importance in the minimization procedure.

These figures show two important results. The first one is the ability of the generalized inertia relief correction to represent the transmitted load from a structure to another when the coupling interface is small. The assumption of a generalized rigid body motion of the interface is then verified, since the MAC for almost all the first twenty one coupled modes are at least 98 %. The relative errors are acceptable when the flexibilities associated to the FE model are used. The second result is the efficiency of the minimization process, since optimum results show even better agreement with the reference results. Only the modes shapes fifteen sixteen exhibit smaller MAC values, still at a reasonable level (more than 80 %, for 164 sensors) and the relative errors for the frequencies are less than 1%. The last coupled mode presented here has a frequency of 14768 Hz, hence almost all the modes shapes in the bandwidth of interest are accurately predicted. The combination of *a priori* shape definition and scaling procedure lead to a efficient reduced model of the active component.

### 4.3 Reconstruction of the interface load $f_0$ .

The second step of the process is the estimation of the interface load  $f_0$  transmitted by the active device to the test structure. In operation measurements have been simulated on the test mesh represented figure 3. Measurements defined at sensors are expanded on the calculated modes shapes  $\Phi^{\&0}$  of the assembled structure  $\Omega + \Omega_0$ . The number of modes shapes used for the reconstruction is an important parameter of the study. The results for three bases are presented on the figure 5.

The choice of a good expansion basis is a key issue in the load estimation procedure. The three bases retained for this example correspond to following cut frequencies :

- around 10 kHz when 16 modes are retained,
- 15 kHz when 23 modes are retained,
- respecting the Rubin criteria, hence around 23 kHz. This is the full coupled basis using the optimized reduced model.

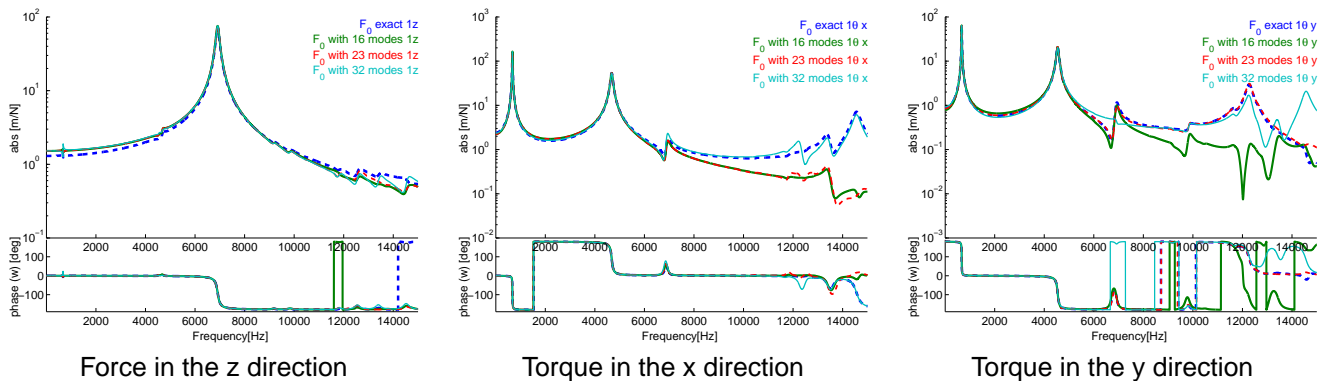


Figure 5: Force and torque ( $f_0$ ) reconstruction, depending on the size of the expansion basis based on  $\Phi^{\&0}$ .

Obviously, the first case cannot provide good results for every direction, since the complete behaviour cannot be represented using this basis. However, considering the force in the z direction, the most important mode is represented in this basis, yielding to a really good estimation of the load. Using a larger expansion basis would only slightly increase the quality of the estimation.

However, considering the other directions, a good estimate for the overall behaviour can drastically increase the quality of the result. Torques along the x and y direction are well estimated, but for two different bases. The largest basis allows a good estimate of the torque along the x direction, but leads to an over estimate of the higher frequency effects in the y direction. Respectively, the medium sized basis is well suited to estimate the effects in the

y direction, but strongly underestimates the effects in the x direction. An explanation comes for the dynamics of the test device. Considering its dimensions, modes in the x and y direction are only lightly coupled, and small errors in the expansion process can lead to strong misestimating in directions where displacements are small. A solution to this issue is the *a priori* selection of the modes shapes inducing loads either in the x direction or in the y direction. Such a regularising process could lead to more accurate results.

#### 4.4 Reconstruction of the equivalent load $f_1$

At this stage, a statically complete model of the active component is available, and the equivalent load  $f_0$  at the interface between the test device and the active component is defined. One can then estimate, with respect to the equation (22), the generalized equivalent load  $\tilde{f}$  to be applied to the active device, coupled with any structure. In order to validate the accuracy of the reconstruction, estimated load  $\tilde{f}$  is applied to the assembled model  $\Omega + \Omega_1$ , and the equivalent interface load  $f_1$  between the active component and the target structure is computed. Results for the three same sizes of the basis  $\Phi^{\&0}$  are presented on the figure 6.

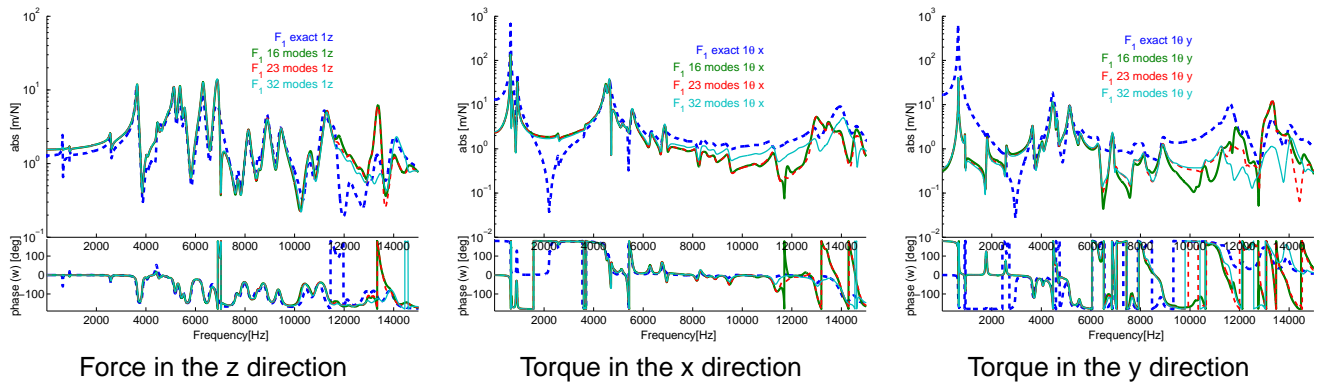


Figure 6: Equivalent force and torque ( $f_1$ ) reconstruction, depending on the size of the expansion basis based on  $\Phi^{\&0}$ .

These results confirm the good behaviour of the proposed methodology to estimate the main load. Effects in the z-direction are fairly well estimated, for all the bases, assuming that the governing mode, around 7500 Hz, is used to estimate  $f_0$ . However, the other effects are not that well represented. The shape of the torque along the x-direction is correctly estimated, but its amplitude is lowered by an average factor of two at medium and high frequencies. In the y-direction, the estimation is correct only over a really limited bandwidth. Considering the shape of the coupled structure, it is clear that both torques along x and y directions, and loads in the z direction could induce very similar responses. Hence, torque misestimation can lead to inaccuracy for in-operation prediction.

Nevertheless, these relatively poor results in the other directions than the z one can be explained with the assumption made in the beginning. Indeed, a strong assumption of generalized rigid body interface behaviour has been made to model the joint between the active structure and the test device. This assumption is verified for these two structures, but it is not the case for the target structure. Coupled modes shapes for the assembled structure using the optimal reduced model of the active device, and a statically complete model of the target structure are not well predicted, due to inaccurate interface behaviour. Hence, the reconstruction of  $f_1$  is biased. This effect is illustrated by the figure 7, detailing the interface behaviour for the complete model (left), and the reduced

model (right). The scaling factor are the same for the first two figures, and is multiplied by ten for the differential displacement.

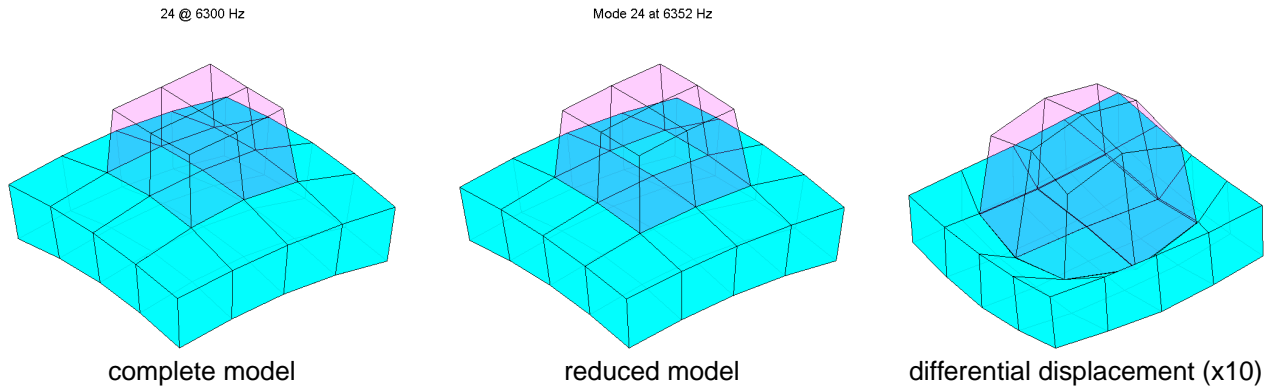


Figure 7: Interface behaviour for a same modeshape. Stiffening due to the generalized motion hypothesis.

The assumption of a generalized rigid body motion of the interface slightly stiffen the interface, hence biasing the prediction results. The accuracy of this assumption should then be verified using the FE model of the target structure. Enriching the interface behaviour in the coupling process would significantly increase the quality of the results. However, this will enlarge the generalized correction shape basis, hence increasing the difficulty to scale these shapes.

## 5 Conclusion

A method has been presented to estimate an equivalent load applied by an active component on a given target structure using both numerical and experimental results. The active component is available, but its behaviour is unknown, and no model exists. A fine FE model of the target structure is available, but the lack of a real structure prevent experimental analysis. Hence, a test device is introduced to fill the gap between the structures.

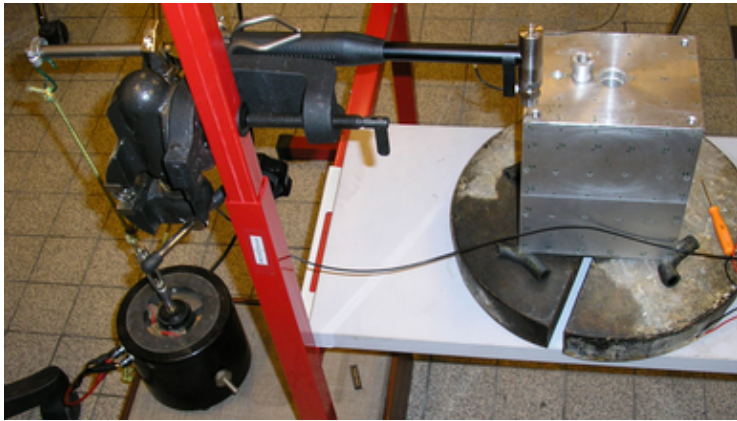
The first step is the set up of a model of the active component. It is modelled using tests results in various configurations, with the help of the well known test device. Combination of modal analysis, model reduction, data expansion and component model synthesis techniques allow the definition of a statically complete reduced model of the active component.

In a second step, in operation measurements on the test assembled structure (test device + active component) allow the computation of a equivalent interface load. Relationships on both test assembled model and target assembled model (target structure + active component) lead to the definition of an equivalent force to be applied on the target structure. This equivalent load represents the dynamic behaviour of the active component, along with its internal loading.

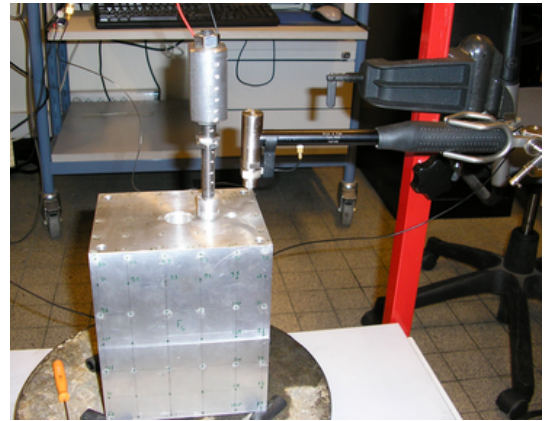
A numerical example has been presented to illustrate the complete methodology. Very good results are obtained for the experimental model of the active component and the identification of the equivalent load between the test device and the active component. Limitations associated to the modelling of the joint are also presented, leading to a less accurate estimation of the equivalent load between the target structure and the active component. Some indications are given to overcome this limitations.

The next steps are the experimental validation of this methodology using an academic test configuration, and the improvement of the modelling of the joint. A test bed has been machined, along with a simplified model of the

active component and the target structure. Structures are presented on the figure 8. FE models are available, and test are in process.



Test device



Test device & active component

Figure 8: Experimental set-up. Modal analysis of the test assembled model

## References

- [1] M. Geradin and D. Rixen. *Mechanical Vibrations: Theory and Applications to Structural Dynamics*. J. Wiley & Sons, second edition, 1997.
- [2] W. Heylen, S. Lammens, and P. Sas. *Modal Analysis Theory and Testing*. KUL Press, Leuven, Belgium, 1997.
- [3] S. W. Doebling, L. D. Peterson, and K. F. Alvin. Estimation of reciprocal residual flexibility from experimental modal data. *AIAA Journal*, 34(8):1678 – 1685, 1996.
- [4] K. F. Alvin and K. C. Park. Extraction of substructural flexibility from global frequencies and modeshapes. *Office of Scientific & Technical Information*, June 1999.
- [5] L. Hermans, P. Mas, W. Leurs, and N. Boucart. Estimation and use of residual modes in modal coupling calculations : a case study. *IMAC XVII*, pages 930 – 936, 1999.
- [6] M. R. Ashory and D. J. Ewins. Generation of the whole frf matrix from measurements on one column. *IMAC XVI*, pages 800 – 814, 1998.
- [7] M. Corus and E. Balmes. *A priori* verification of local fe model based force identification. *ISMA*, 2004.
- [8] E. Balmes. Use of generalized interface degrees of freedom in component mode synthesis. *IMAC*, pages 204–210, 1996.
- [9] M. Corus, E. Balmes, and O. Nicolas. Using model reduction and data expansion techniques to improve sdm. *Mechanical Systems and Signal Processing*, 2005.
- [10] R. R. Craig and M. C. Bampton. Coupling of substructures for dynamic analyses. *AIAA Journal*, 6(7):1313 – 1319, 1968.